CHAPTER 3

EXPERIMENTAL METHODS

3.1 Introduction

Four different systems were prepared i.e. PEO –LiI salt, PEO-LiI- Al_2O_3, PEO-LiI-Calix4 and PEO-LiI-Calix6. Characterization of the polymer electrolytes in this thesis will be carried out using the techniques discussed in this chapter.

Several techniques have been employed to identify the characteristics of the PEO based polymer electrolyte. These techniques include Fourier transform infrared spectroscopy (FTIR), x-ray diffraction (XRD) and electrochemical impedance spectroscopy (EIS).

3.2 Sample Preparation

The polymer electrolytes in this study were prepared by the solution casting method. In the present investigation, the polymer is poly(ethylene oxide) (PEO), average MW ~ 10^7 (Aldrich). The inorganic salt LiI and inorganic filler Al_2O_3 and the organic macromolecule Calix4, and Calix6 were taken in different stoichiometric ratios. Both PEO and Lithium Iodide of molar mass of 133.845 g/mol were purchased from Aldrich. Both solvents Acetonitrile and Isopropyl Alcohol were procured from J.T Baker, Calix4 molecular formula of $C_{28}H_{24}O_4$, molecular weight of 424.496 and for calix6 arenes molecular formula of $C_{42}H_{36}O_6$ and molecular weight of 636.76 from Aldrich and the filler Aluminium Oxide of molar mass 101.961 g/mol from Unilever. All the materials except for the salts were used without further purification.

Figure 3.1 depicts the structure of (a) Calix4 arenes and (b) Calix6 arenes. Calixarenes are characterised by a three-dimensional basket, cup or bucket shape. Calixarenes are characterised by a wide upper rim and a narrow lower rim and a central annulus. In calix4 4 hydroxyl groups and in calix6 6 hydroxyl groups are intrannular on the lower rim.

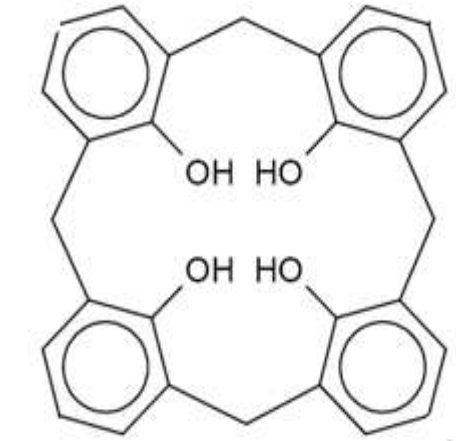

(a)

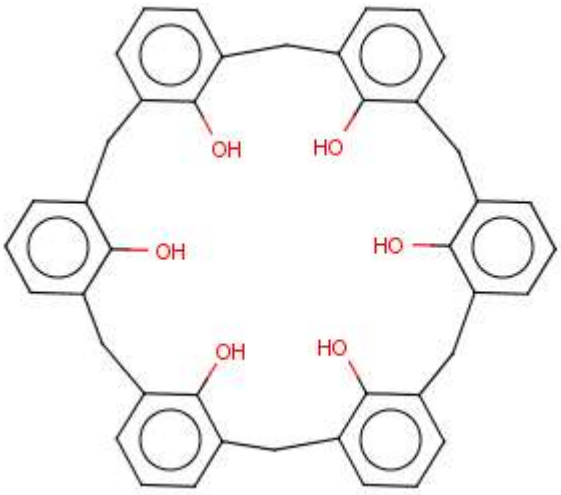

(b)

Figure 3.1: (a) Structure of calix4 arene molecule and (b) structure of calix6 arene molecule

3.2.1 Preparation of PEO-LiI system

The solutions were mixed and stirred in Acetonitrile solution for few hours at room temperature to ensure complete dissolution. The solutions were then cast in different petri dishes and allowed to dry at room temperature. After several days, the films were further dried by keeping them in a dessicator before characterization was carried out on them. In Table 3.1 shows the weight percentages of PEO and LiI used to prepare the film.

Table 3.1: Compositions of PEO:LiI

PEO (wt%)	LiI (wt%)
96	4.00
94	6.00
92	8.00
90	10.00
88	12.00
86	14.00

Figure 3.2 shows the flow chart for the preparation of PEO-LiI electrolyte system.

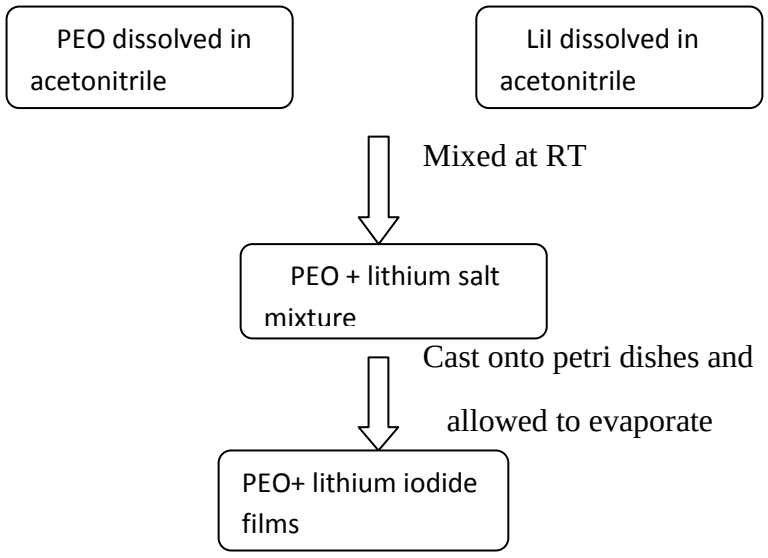

Figure 3.2: Flow diagram for the preparation process of PEO-LiI electrolyte systems.

3.2.2 Preparation of PEO-LiI-Al_2O_3 system

It was found that PEO exhibited the highest ambient temperature conductivity at 10 wt.% LiI added. Based on this result, the inorganic filler Al_2O_3 is mixed with the PEO-LiI system at different wt.% as shown in Table 3.2. Table 3.2 summarizes the compositions of the prepared system.

Table 3.2: Compositions of PEO:LiI: Al_2O_3

PEO (wt.%)	LiI (wt.%)	Al_2O_3(wt.%)
85.50	9.50	5.00
81.00	9.00	10.00
76.50	8.50	15.00
72.00	8.00	20.00
67.50	7.50	25.00

Prior to mix with PEO-LiI system Al_2O_3 was dissolved in isopropyl alcohol. The dissolved Al_2O_3 is added to the PEO-LiI homogeneous mixture and stirred it for 12 hrs. The solutions were then cast onto different glass Petri dishes and left to dry to form films and then stores in desiccators before further analysis. Figure 3.3 shows a flow chart in the preparation of PEO-LiI-Al_2O_3 system.

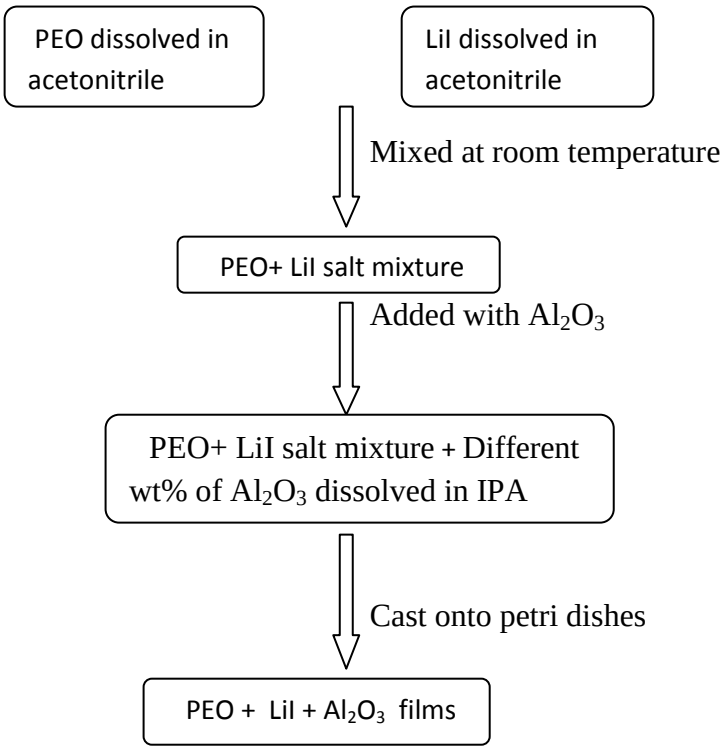

Figure 3.3: Flow diagram for the preparation process of PEO +LiI + inorganic salt Al_2O_3

Figure 3.4, shows the schematic representation of polymer salt system with inorganic filler Al_2O_3.

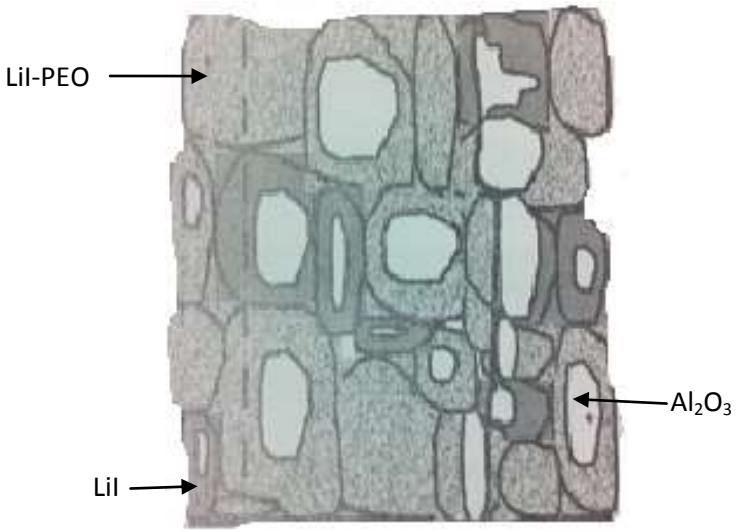

Figure 3.4: Schematic presentation of highly concentrated composite solid polymer electrolytes (Golodnitsky et al., 2002)

3.2.3 Preparation of PEO-LiI- Calix arenes

This system was prepared in order to examine the complexation and thereby anion trapping. To the high conducting PEO-LiI system, different weight percentages of calix arenes dissolved in carbon tetra chloride (CCl_4) solvent were added. The samples were stirred for 12 hrs at room temperature to get the homogeneous solution, which later poured into glass petri dishes and allowed to dry to form films in the dessicator. The weight percentage of the samples prepared is listed in Table 3.3.

Table 3.3: Compositions of PEO:LiI: Calix

PEO (wt%)	LiI (wt%)	Calix (wt%)
89.10	9.90	1
88.20	9.80	2
87.30	9.70	3
86.40	9.60	4
85.50	9.50	5

Figure 3.5 depicts the flow chart for the preparation of PEO-LiI-Calix arenes. After the stirring for 12 hours the homogenous solution is poured into glass petri dishes for drying.

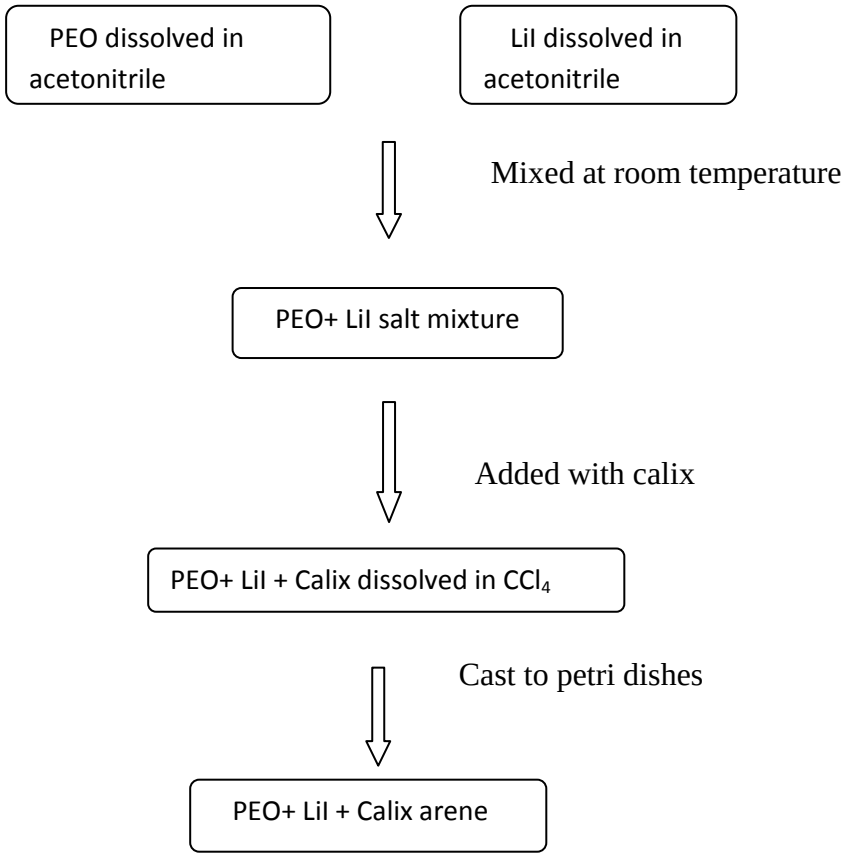

Figure 3.5: Flow diagram for the preparation process of PEO - LiI - Calix

3.3 Fourier Transform Infrared Spectroscopy (FTIR)

The interactions between the polymer hosts, salt(s) and plasticizer can be determined by FTIR studies. FTIR has been employed by many researchers [Majid and Arof (2005); Kumutha and Alias (2006); Ramesh and Chai (2007)] to determine the occurrence of complexation between polymer and salt. In this thesis, infrared spectra of resultant films were recorded using the Thermo Scientific/Nicolet SIO spectrophotometer at ambient temperature in the wavenumber region between 4000 cm^{-1} and 650 cm^{-1} to verify the occurrence of complexation between PEO-LiI, PEO-LiI-Al_2O_3 and PEO-LiI-Calix arenes. The resolution used was 1 cm^{-1}. Figure 3.5 shows FTIR spectra of PEO with LiI and Calix arenes Siekierski et al.,(2009).

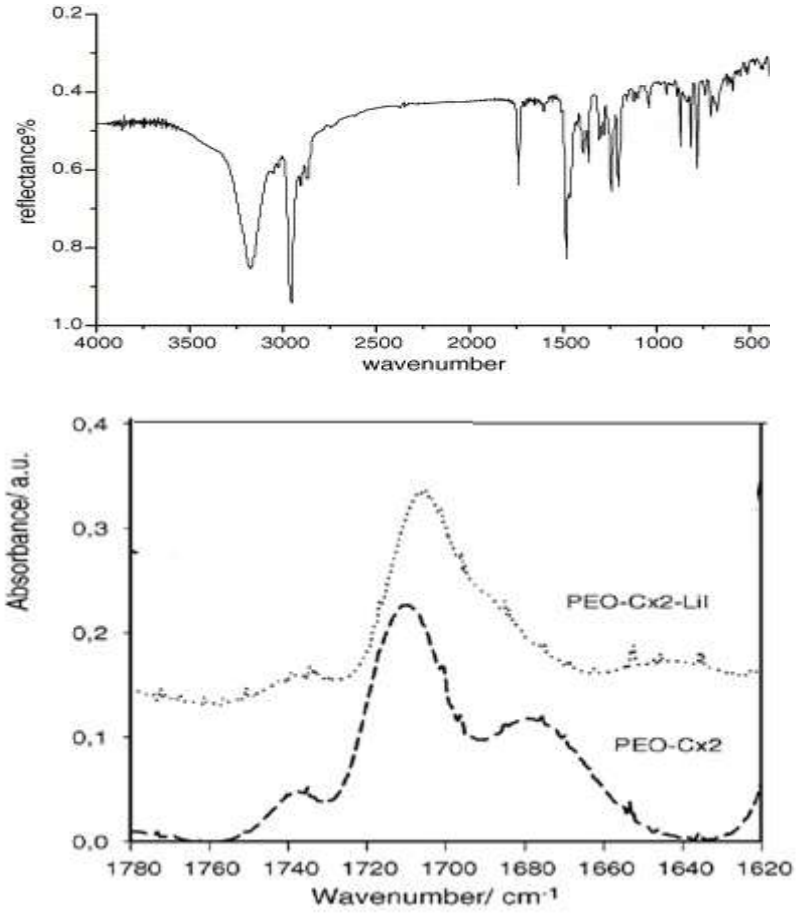

Figure 3.6: FT-IR spectra of PEO membranes doped with calix arenes

Table 3.4 shows FTIR vibrational bands of PEO systems obtained from literature.

Table 3.4: FTIR vibrational bands of PEO systems

Assignment	Wavenumber (cm^{-1})	Reference
I^- Bending of LiI	1620	Pawlowska et al., 2007
ν_s(C-O-C) of PEO	1096 1099	Zuwkowska et al., 2007
CH_2 twisting in PEO	1340	Xi and Tang 2005
C-O stretching	1700	Pawlowska et al., 2007
C-C stretching	1071	Wang et al., 2008
C-H bending	1237	Kalita et al., 2008
CH_3 rocking	1079	Pawlowska et al., 2007
C-H asymmetric Stretching	1726	Sheng-Jen Lin et al., 2009
CH_2 bending	1401	Pawlowska et al., 2007
CH_2 wagging	1344 1359	Wieczorek et al., 2009

3.4 X-ray Diffraction (XRD)

X-ray diffraction (XRD) is an important technique to obtain information up to atomic scale from both crystalline and amorphous materials. By observing the characteristic patterns of the X-ray diffractograms obtained, a material can be determined as crystalline or amorphous. The technique of XRD can be applied to indicate the occurrence of complexation between the polymer host and the dopping salt. Complexation can be indicated by the shifts in peaks, changes in the relative intensities of peaks and existence or absence of peaks in the diffractograms of the samples [Sivakumar et al., 2006, Rajendra et al., 2004, Sreekanth et al., 1999, Reddy et al., 2007].

The diffraction intensity of films was measured using X-ray diffractometer (Siemens D5000) with operating voltage of 40 kV and current of 40 mA. The X-ray wavelength is 1.5406 Å. The X-rays impinge the films at 2 theta angles between 5° and 80°. The glancing angle increased in steps of 0.04°.

As the sample rotates, the angles θ between the incident beam and the normal to the film is changed. X-rays hit the sample but some of the rays are diffracted. X-rays are reflected to the detector when the Bragg condition

$$2d \sin\theta = n\lambda \qquad (3.1)$$

is satisfied. Here d is the inter planar spacing,θ is the Bragg angle, n is the order of diffraction and λ is the wavelength of X-ray. Examples of XRD diffraction patterns of PEO mixed with $LiClO_4$ and nano particle sulphated Zirconia has shown in Figure 3.7. According to Jingyu Xi et al., (2005), the crystalline fractions in samples can be predicted

from the ratio of the integrated intensity of peaks associated with crystalline reflections to the integrated area of the spectrum by equation below.

$$X_c = (A_c/A_T) \times 100 \qquad (3.2)$$

Where Xc is the crystalline fraction, A_T and A_C are the total and crystalline hump areas, respectively. Therefore, the degree of the crystalline fractions can be estimated.

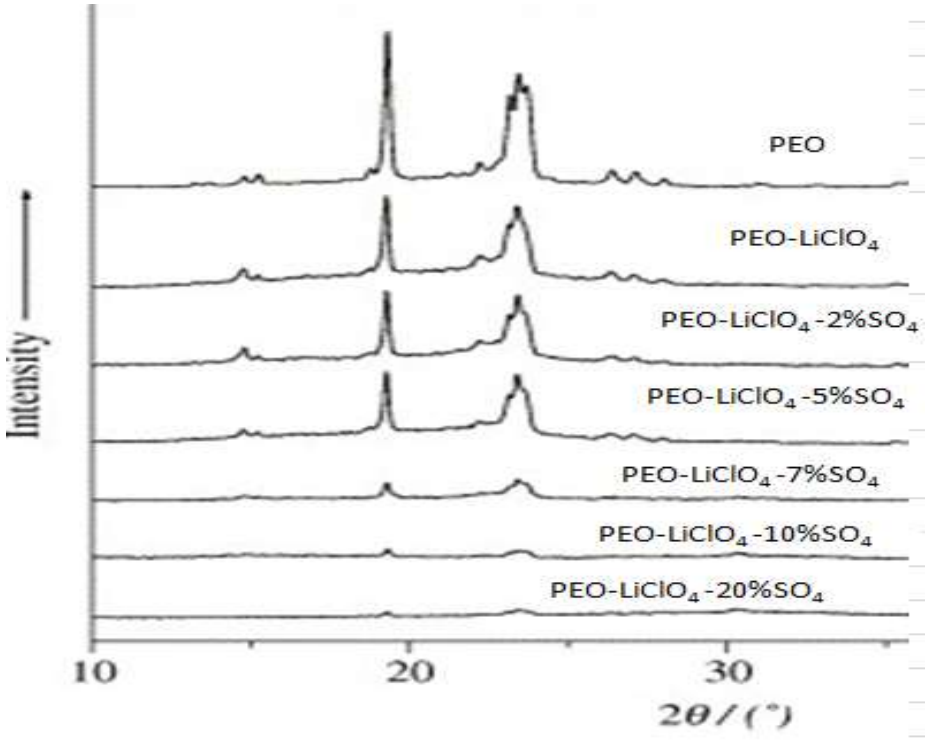

Figure 3.7: XRD diffractogram for pure PEO, PEO-$LiClO_4$, and different weight percentages of sulphated Zircona

Refering to Xi et al., (2005) a rapid decrease of the PEO crystallinity resulting from the coordination interactions between the ether oxygen atoms of PEO and Li^+ (Xi et al., 2005). This is confirmed by Kalita et al., (2007) by suggesting that the intensity of the peak by an addition of lithium salt reduces the PEO crystalline structure.

3.5 Electrochemical Impedance Spectroscopy (EIS)

Impedance measurements of the films were carried out using HIOKI 3531-01 LCR Hi-tester that was interfaced to a computer. The impedance was measured in the frequency range from 50 Hz to 1 MHz in the temperature range from 298K to 373 K. All samples were sandwiched between two stainless steel electrodes with a diameter of 1cm under spring pressure. The conductivity of the films can be calculated using the following equation:

$$\sigma = d / R_b A \qquad (3.3)$$

where *d* is the thickness of the electrolyte and A is the electrolyte-electrode contact area, R_b is the bulk impedance of sample obtained from Cole-Cole plot of negative imaginary impedance versus real impedance.

Other functions in impedance spectroscopy are complex admittance A(w), complex permittivity Ɛ (w) and complex electrical modulus M(w) which can be derived from the impedance data. The relationship between admittance and impedance is given by:

$$A(w) = \frac{Z'}{(Z'^2+Z''^2)} - \frac{jZ''}{(Z'^2+Z''^2)} \qquad (3.4)$$

The relationship between complex permittivity and impedance is given by:

$$\varepsilon(w) = \frac{Z''}{\omega C_0 (Z'^2 + Z''^2)} + \frac{jZ''}{\omega C_0 (Z'^2 + Z''^2)} \qquad (3.5)$$

The relationship between modulus and complex permittivity is given by

$$M(w) = \frac{\varepsilon'}{(\varepsilon'^2+\varepsilon''^2)} - \frac{j\varepsilon''}{(\varepsilon'^2+\varepsilon''^2)} \quad (3.6)$$

The loss tangent equation can be written as,

$$\tan\delta = \frac{M''}{M'} \quad (3.7)$$

Or $$\tan\delta = \frac{\epsilon''}{\varepsilon'} \quad (3.8)$$

The terms in equations stated above is defined as follows;

$w = 2\pi f$ (angular frequency)

C_0 = Vacuum capacitance of the empty cell

$Z' = Z\cos\theta$

$Z'' = Z\sin\theta$

$j = \sqrt{-1}$

The electrical conductivity for each sample was measured six times for each sample prepared.

In Figure 3.8,Arup Dev et al., (2010) have studied the conductivity of PEO with $LiClO_4$ and different weight percentages of CeO_2. In the impedance analysis it is showed that the PEO electrolyte is thermally assisted and interestingly the samples exhibit Arrhenius conductivity- temperature relationship in the temperature range between 298 K to 333 K.

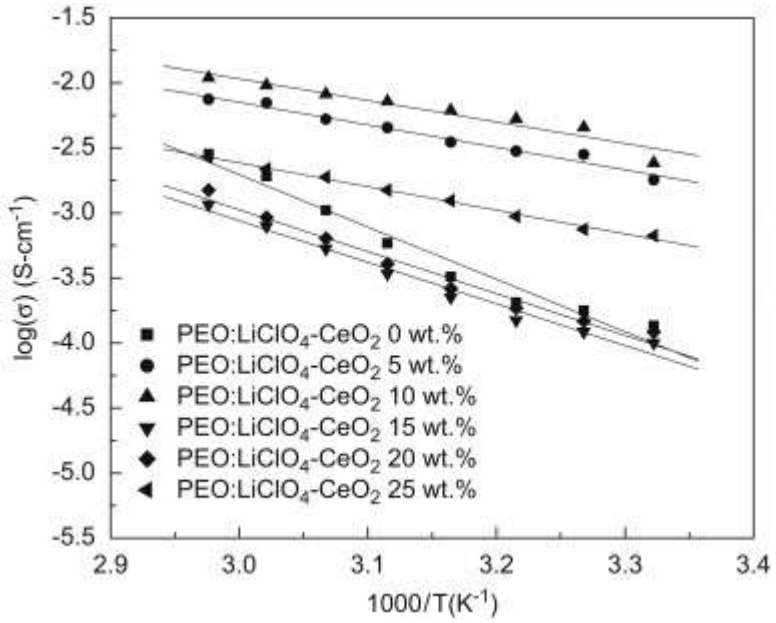

Figure 3.8: Arrhenius plot of the PEO:$LiClO_4$-CeO_2 at different weight percentages at different temperatures [Arup Dev et al., 2010]

Figure 3.9, [Subba Reddy et al., (2007)] show that Cole-Cole plot of PEO may consist of a titled spike or semicircle followed by a spike tail even in the highly plasticizer condition. In the complex impedance representation, the low frequency response appears as an inclined spike and such a spike (tail-like) is characteristic of a blocking double-layer capacitance. The high frequency semicircle corresponds to the bulk response of the films. These results suggest that the migration of ions may occur through the volume of matrix polymer, which can be represented by a resistor. The immobile polymer chains, on the other hand, become polarized in the alternating field, and can therefore be represented by a capacitor. The ionic migration and bulk polarization are physically in parallel, and therefore, the portion of the semicircle can be observed at high frequencies [Subba Reddy et al., (2006)].

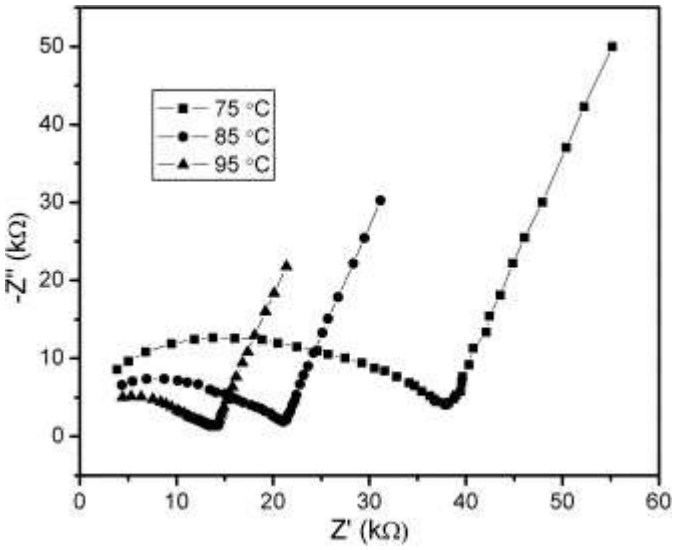

Figure 3.9: The Cole-Cole plots of PEO +$LiClO_4$+ CeO_2

3.6 Summary

Results and discussion which conducted using the above mentioned methods will be discussed in the following chapter